

Received December 25, 2018, accepted January 16, 2019, date of publication January 24, 2019, date of current version February 12, 2019.

Digital Object Identifier 10.1109/ACCESS.2019.2894911

An Adaptive Sliding Mode Control With Effective Switching Gain Tuning Near the Sliding Surface

SEUNGMIN BAEK¹, JAEMIN BAEK², (Member, IEEE),
AND SOOHEE HAN¹, (Senior Member, IEEE)

¹Department of Creative IT Engineering, Pohang University of Science and Technology, Pohang 37673, South Korea

²Agency for Defense Development, Daejeon 34186, South Korea

Corresponding author: Soohee Han (soohee.han@postech.ac.kr)

This work was supported in part by the Sports Promotion Fund of Seoul Olympic Sports Promotion Foundation, Ministry of Culture, Sports and Tourism, under Grant 1375026841, and in part by the Human Resources Program in Energy Technology, Korea Institute of Energy Technology Evaluation and Planning, Ministry of Trade, Industry and Energy, under Grant 20174030201660.

ABSTRACT This paper proposes a new adaptive law for a sliding mode control (SMC) scheme to achieve the effective switching gain tuning near the sliding surface. The proposed adaptive law makes the switching gains rapidly and effectively decrease near the sliding surface to provide the well-functioning adaptation while avoiding the sign changes caused by excessive adaptation. Such an adaptation mechanism contributes to chattering reduction and fast adaptation of the switching gains without temporary large tracking errors. The proposed adaptive SMC (ASMC) works together with a time-delay controller (TDC) for a more practical implementation based on a model-free controller. Fortunately, the proposed ASMC has an additional benefit of suppressing time-delay estimation errors inherently arising from the TDC. In other words, the proposed ASMC acts in synergy with the TDC. The simulations are performed, and the comparisons are made with the existing control schemes to illustrate the good tracking performance of the proposed ASMC. These simulations have shown that with a 2 degree-of-freedom robot manipulator, the proposed ASMC has a good nominal and robust performance with a very strategic adaptive law.

INDEX TERMS Adaptive sliding mode control (ASMC), time-delay controller (TDC), time-delay estimation (TDE), adaptation, robot manipulators.

I. INTRODUCTION

Sliding mode control (SMC) is well known as an effective nonlinear control scheme under model uncertainties and unknown external disturbances. Many control applications have been developed with SMCs, which include electromechanical systems [1], inverted pendulum systems [2], and robot manipulators [3], to enhance robustness against various uncertainties arising from real systems. Such practical SMCs require large switching gains to achieve robustness to uncertainties with known bounds and, hence, tend to suffer from chattering that reduces the performance and degrades the actuators. Improved versions have been developed with high-order SMC [4], [5], continuous SMC [6], [7], low-pass filtering [8], [9], and so on to mitigate undesirable chattering. As a more flexible method, switching gains of SMCs were not fixed, but made variable adaptively without knowledge on an upper bound on uncertainties.

Adaptive SMC (ASMC) schemes have been developed to employ well-timed adaptive switching gains depending

on the tracking errors and overcome the chattering problem in a more fundamental way [10]–[12]. These ASMCs adjust their switching gains online without regard to an upper bound on the unknown model uncertainties and external disturbances. However, in real systems, they still have chances of inducing chattering by monotonically increasing switching gains [10] and providing the slow adaptation speed of the switching gains [11], [12]. As another approach to resolving issues on chattering and slow adaptation speed, ASMCs have been developed to ensure finite time convergence and perform high-precision control with a fast response [13]–[15]. However, some problems have not yet been solved by these approaches. Chattering still occurs because of non-decreasing switching gains [13], [14]. Moreover, the inefficient management between performance and chattering results from the estimated upper bounds of uncertainties and disturbances [15]. The adaptive law depending on the sliding variables is proposed, which makes the derivatives of the switching gains inversely proportional to them near the

sliding surface [16], to effectively handle the trade-off between performance and chattering without respect to the magnitudes of uncertainties and disturbances. It makes switching gains rapidly decrease near the sliding surface, such that a fast adaptation speed can be achieved, and chattering is alleviated. Theoretically, this adaptive law is very ideal for a good tracking performance with less chattering and a fast adaptation speed, which can be confirmed in simulation studies or in a good hardware environment.

From a practical implementation perspective, a theoretically proven fast adaptation of the switching gains near the sliding surface is difficult to obtain in a cost-effective hardware environment with insufficient computing power. Adaptive switching gains may provide excessive change if the sampling time is not sufficiently small because of limited computing capability; hence, their signs may change in recomputing them for the next step near the sliding surface, which temporarily leads to large tracking errors. Employing additional parameters and making the derivatives of switching gains proportional to the sliding variables at the sacrifice of chattering reduction and fast adaptation speed have been tried to deal with such improper adaptation [17]. In this regard, developing a new type of ASMC that achieves both fast adaptation speed and chattering reduction without improper excessive adaptation would be practically meaningful.

This study proposes a new adaptive law for ASMC to provide effective fast adaptation near the sliding surface and reduce chattering with proper adaptation. The proposed adaptive law adjusts the switching gains in the vicinity of the sliding surface to achieve fast adaptation and chattering reduction while avoiding excessive adaptation. According to the adaptive law, the sliding variables move toward and stay in an arbitrarily small vicinity of the sliding surface. Away from the sliding surface, the derivatives of the switching gains are proportional to the magnitudes of the sliding variables, which guarantees robustness without information on the upper bounds of uncertainties. In the vicinity of the sliding surface, they are proportional to the negative exponential of the magnitudes of the sliding variables, which contributes to chattering reduction and fast adaptation of switching gains without temporary large tracking errors caused by excessive adaptation. For this reason, the proposed ASMC could be said to have a good tracking performance even in a cost-effective hardware environment with a relatively large sampling period. For a more practical implementation based on a model-free controller, the proposed adaptive SMC (ASMC) works together with a time-delay controller (TDC) [18], [19]. Fortunately, the proposed ASMC has an additional benefit of suppressing the time-delay estimation (TDE) errors inherently arising from the TDC [20]–[23]. In other words, the proposed ASMC acts in synergy with the TDC. The tracking errors of the proposed ASMC are uniformly and ultimately bounded (UUB) using a Lyapunov approach. Simulations are performed, and comparisons are made with existing control schemes to illustrate the good tracking performance of the

proposed ASMC. These simulations have illustrated that with a 2 degree-of-freedom (DOF) robot manipulator, the proposed ASMC has a good nominal and robust performance with a very strategic adaptive law.

This paper is organized as follows: Section II briefly introduces the TDC for a general uncertain nonlinear multi-input multi-output (MIMO) system; Section III presents the design of the ASMC for general nonlinear MIMO systems with effective switching gain tuning near the sliding surface, and depicts the performed simulations and the comparisons made with the existing control schemes; and finally, Section IV concludes the study with a brief summary of this paper.

II. TIME-DELAY CONTROL

The dynamics of an uncertain nonlinear MIMO system can be described as follows:

$$\ddot{\mathbf{x}}_t = \mathbf{f}_t + \mathbf{g}_t + \mathbf{b}_t \mathbf{u}_t \quad (1)$$

where $\mathbf{x}_t = [\ddot{x}_{1,t}, \ddot{x}_{2,t}, \dots, \ddot{x}_{n,t}]^T \in \mathfrak{R}^n$ is the state variable; $\mathbf{f}_t = [f_{1,t}, f_{2,t}, \dots, f_{n,t}]^T \in \mathfrak{R}^n$ and $\mathbf{b}_t = [b_{1,t}, b_{2,t}, \dots, b_{n,t}] \in \mathfrak{R}^n \neq 0$ are the known nonlinear functions; $\mathbf{g}_t = [g_{1,t}, g_{2,t}, \dots, g_{n,t}] \in \mathfrak{R}^n$ is the unknown bounded disturbance satisfying $\|\mathbf{g}_t\| \leq l_g$ for $l_g > 0$; and $\mathbf{u}_t = [u_{1,t}, u_{2,t}, \dots, u_{n,t}] \in \mathfrak{R}^n$ is the control input.

The system model (1) can be compactly expressed as follows:

$$\ddot{\mathbf{x}}_t = \mathbf{h}_t + \bar{\mathbf{b}}^{-1} \bar{\mathbf{u}}_t \quad (2)$$

where $\mathbf{h}_t = \bar{\mathbf{b}}^{-1}[\mathbf{b}_t^{-1}(\mathbf{f}_t + \mathbf{g}_t) + (\bar{\mathbf{b}} - \mathbf{b}_t^{-1})\ddot{\mathbf{x}}_t] \in \mathfrak{R}^n$, and $\bar{\mathbf{b}} \in \mathfrak{R}^{n \times n}$ is a constant diagonal matrix to be determined later on.

The control objective herein is to steer the state \mathbf{x}_t along the desired state $\mathbf{x}_{d,t} \in \mathfrak{R}^n$, which means that the tracking error $\mathbf{e}_t = \mathbf{x}_{d,t} - \mathbf{x}_t \in \mathfrak{R}^n$ should be as close as possible to zero. \mathbf{h}_t is unknown; hence, we use its estimate $\hat{\mathbf{h}}_t$ that will be discussed later on. The TDC is constructed as follows:

$$\bar{\mathbf{u}}_t = -\bar{\mathbf{b}}\hat{\mathbf{h}}_t + \bar{\mathbf{b}}(\ddot{\mathbf{x}}_{d,t} + \mathbf{K}_d \mathbf{e}_t) \quad (3)$$

where $\mathbf{K}_d = \text{diag}(k_{s1}, k_{s2}, \dots, k_{sn}) \in \mathfrak{R}^{n \times n}$ is a positive matrix designed for guaranteeing stability.

As a simple estimate of \mathbf{h}_t , $\hat{\mathbf{h}}_t$ in (3) can be obtained from its one-sample time-delayed measurement as follows:

$$\hat{\mathbf{h}}_t \triangleq \mathbf{h}_{t-L} \quad (4)$$

where L is called a time delay constant that is often taken to be a sampling time period for easy implementation. We obtained the following from a system model (2) and the TDE (4):

$$\mathbf{h}_{t-L} = \ddot{\mathbf{x}}_{t-L} - \bar{\mathbf{b}}^{-1} \bar{\mathbf{u}}_{t-L} \quad (5)$$

It then follows that putting (3)–(5) together yields:

$$\bar{\mathbf{u}}_t = -\bar{\mathbf{b}}\ddot{\mathbf{x}}_{t-L} + \bar{\mathbf{u}}_{t-L} + \bar{\mathbf{b}}(\ddot{\mathbf{x}}_{d,t} + \mathbf{K}_d \dot{\mathbf{e}}_t) \quad (6)$$

By substituting the control input (6) into (2), the system model (2) can be rewritten as follows:

$$\ddot{\mathbf{e}}_t + \mathbf{K}_d \dot{\mathbf{e}}_t + \mathbf{h}_t - \mathbf{h}_{t-L} = 0 \quad (7)$$

If the constant gain matrix $\bar{\mathbf{b}}$ in (2) is chosen to satisfy the following condition [24]

$$\|\mathbf{I} - \mathbf{b}_t \bar{\mathbf{b}}\| < 1 \tag{8}$$

for all $t \geq 0$, then the TDE error or $\mathbf{h}_t - \hat{\mathbf{h}}_t = \mathbf{h}_t - \mathbf{h}_{t-L}$ is bounded by a positive constant value denoted by $\bar{\mathbf{h}}^* = [\bar{h}_1^*, \bar{h}_2^*, \dots, \bar{h}_n^*]$ and the stability is also guaranteed by the boundedness of the TDE errors. Furthermore, It is easier to choose $\bar{\mathbf{b}}$ to be smaller to satisfy the above condition (8), but TDE errors will become larger and more dynamic. This is another reason ASMC is needed.

In the following section, the ASMC with effective switching gain tuning near the sliding surface will be designed based on the above-mentioned model-free TDC.

III. ASMC WITH EFFECTIVE SWITCHING GAIN TUNING

A. CONTROL DESIGN

The sliding variable s_t is designed as follows:

$$s_t = \dot{e}_t + K_s e_t \tag{9}$$

where $s_t = [s_{1,t}, s_{2,t}, \dots, s_{n,t}]^T \in \mathfrak{R}^n$, and $K_s = \text{diag}(k_{s1}, k_{s2}, \dots, k_{sn}) \in \mathfrak{R}^{n \times n}$ is a positive matrix designed for adjusting the convergence rate.

Using the sliding variable s_t in (9), we propose the following ASMC based on the TDC:

$$\begin{aligned} \ddot{u}_t = & -\bar{\mathbf{b}}\ddot{x}_{t-L} + \ddot{u}_{t-L} \\ & + \bar{\mathbf{b}}(\ddot{x}_{d,t} + K_s \dot{e}_t + K_p s_t + \hat{K}_t \text{sgn}(s_t)) \end{aligned} \tag{10}$$

where $K_p = \text{diag}(k_{p1}, k_{p2}, \dots, k_{pn}) \in \mathfrak{R}^{n \times n}$ and $\hat{K}_t = \text{diag}(\hat{k}_{1,t}, \hat{k}_{2,t}, \dots, \hat{k}_{n,t}) \in \mathfrak{R}^{n \times n}$ are positive matrices to be determined later on. Note that the switching gain \hat{K}_t plays a role in suppressing the disturbances and uncertainties. Its adaptive law is proposed as follows:

$$\hat{k}_{i,t} = \begin{cases} \varphi_i \left\{ \gamma_i^{-1} \right\}^{\theta_t} \left(\underbrace{|s_{i,t}|}_{\text{For large } |s_{i,t}|} + \underbrace{\beta_i e^{-|s_{i,t}|}}_{\text{For small } |s_{i,t}|} \right) \cdot \theta_t & \text{if } \hat{k}_i > 0 \\ \varphi_i \gamma_i^{-1} (|s_{i,t}| + \beta_i e^{-|s_{i,t}|}) & \text{if } \hat{k}_i = 0 \end{cases} \tag{11}$$

where φ_i , γ_i , and β_i are positive gains for adjusting the adaptation speed, and θ_t is given by $\text{sgn}(\|s_t\|_\infty - \varepsilon)$ for a positive ε . The Appendix shows that ε affects the ultimate bound of the sliding variable $s_{i,t}$.

As seen in the proposed adaptive law (11), the information on the upper bounds of uncertainties and disturbances are not required. Furthermore, two terms $|s_{i,t}|$ and $\beta_i e^{-|s_{i,t}|}$ in (11) are dominant for large and small $|s_{i,t}|$, respectively. In other words, the proposed adaptive law has two gain terms, whose dominance are alternated according to the magnitude of the sliding variable.

- **For large** $\|s_t\|_\infty$ or $\|s_t\|_\infty \geq \varepsilon$

When the magnitude of the i -th component of s_t , or $|s_{i,t}|$, is far away from zero and larger than ε , $|s_{i,t}|$ is dominant over $\beta_i e^{-|s_{i,t}|}$ in the adaptive law (11) since $\beta_i e^{-|s_{i,t}|}$ is almost zero. The derivatives of the switching gains $\hat{k}_{i,t}$

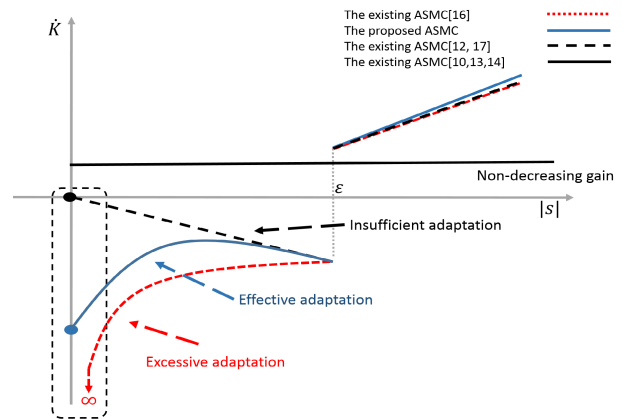


FIGURE 1. Comparison of adaptive laws near the sliding surface.

are highly affected by $|s_{i,t}|$ and hence they increase for fast convergence until $|s_{i,t}|$ reaches the vicinity of the sliding surface, or $\|s_t\|_\infty < \varepsilon$. This adaptive mechanism makes $|s_{i,t}|$ smaller than ε rapidly and hence provides the good tracking performance in the transient response.

- **For small** $\|s_t\|_\infty$ or $\|s_t\|_\infty < \varepsilon$

Consider the case where, for $i = 1, \dots, n$, $|s_{i,t}|$ are less than ε and close to zero. In this case, the switching gain should be as small as possible to reduce chattering. However, the chattering problem may be caused since it takes time to decrease high switching gains with small $|s_{i,t}|$. For this purpose, $\beta_i e^{-|s_{i,t}|}$ is added in the adaptive law (11), which is dominant over $|s_{i,t}|$ near the sliding surface since $|s_{i,t}|$ is almost zero. It is noted that $\beta_i e^{-|s_{i,t}|}$ does not vanish, but increases as $|s_{i,t}|$ goes to zero. Since the adaptive law (11) is highly affected by $\beta_i e^{-|s_{i,t}|}$, it guarantees the fast decreasing speed of switching gains and achieves good steady-state performance near the sliding surface. Since $\beta_i e^{-|s_{i,t}|}$ is upper bounded, excessive adaptation arising from existing schemes can be also avoided.

The tuning method is described step by step as follows:

Step 1) Choose a proper β_i in consideration of the sampling time. As the sampling time becomes large, β_i should increase.

Step 2) Fix φ_i and γ_i in consideration of increasing and decreasing speeds of the switching gains. For fast increasing switching gains, φ_i should be large and γ_i should be small. For fast decreasing switching gains, φ_i should be small and γ_i should be high. Practically, such trade off should be settled.

Step 3) Repeat Step 1) and Step 2) once again if the tracking performance does not reach a desired level.

Fig. 1 shows a graphical comparison of the adaptive laws of the proposed and existing ASMCs. The derivatives of the switching gains in [10], [13], and [14] are taken to be constant, which may induce chattering as mentioned earlier. In the case of the existing ASMCs [12], [17], the switching gains decrease at the rate proportional to the magnitude of the sliding variable near the sliding surface. It takes time

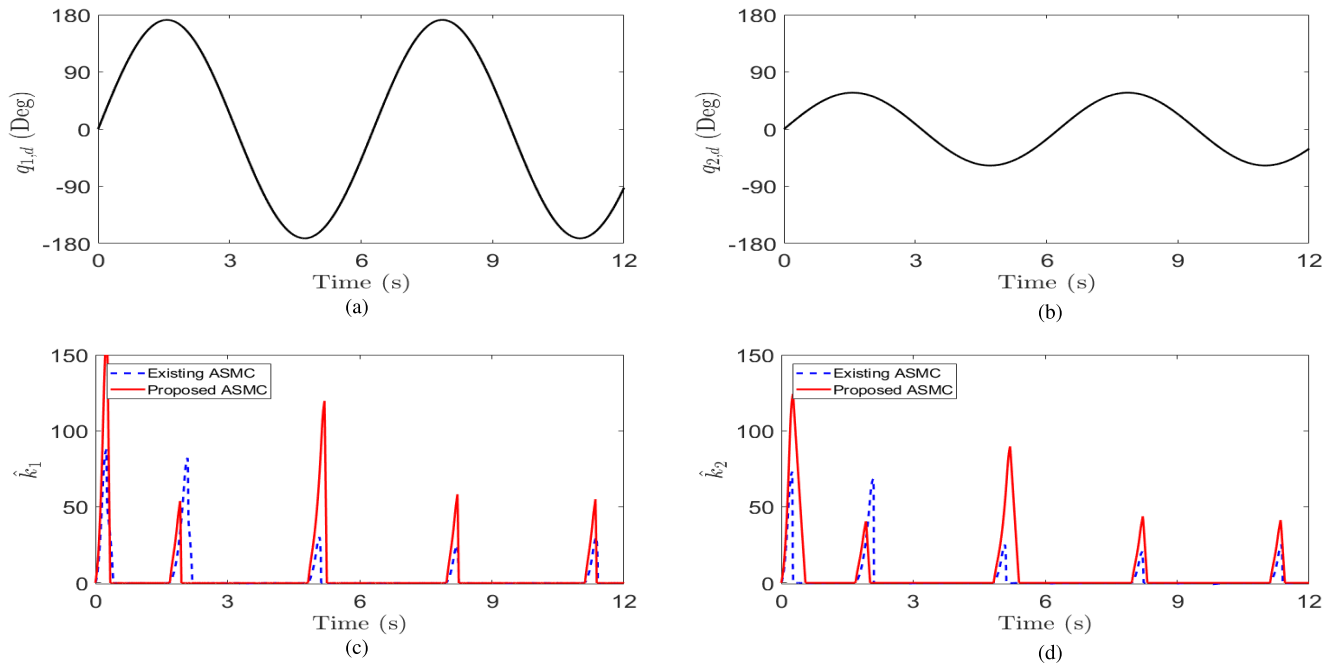


FIGURE 2. Comparison of the switching gains for the given reference angles in the joint space without payload: (a) reference angle of joint 1, (b) reference angle of joint 2, (c) switching gains of the proposed and existing ASMCs for joint 1, and (d) switching gains of the proposed and existing ASMCs for joint 2.

to decrease high switching gains with small $|s|$; therefore, temporary chattering can be observed because of insufficient adaptation. Very high switching gains can be employed to solve such insufficient adaptation problems [16]. However, as shown by the dotted line in Fig. 1, \hat{K} diverges and switching gains become negative as $|s|$ goes to zero. If the sampling time is not sufficiently small due to limited computing capability and hardware limitation, adaptive switching gains may provide excessive change and hence their signs may change in recomputing them for the next sampling time point near the sliding surface, which leads to large tracking errors temporarily.

In the case of the proposed ASMC, the decreasing speed is controllable because the derivative of switching gain has constant value at the sliding surface due to the exponential term. It implies that we can control the sensitivity of switching gain to sliding variable near the sliding surface. The solid line in Fig. 1 illustrates that the adaptive law of the proposed ASMC achieves a compromise between insufficient and excessive adaptation. The adaptation speed of the proposed ASMC has enough power to keep $|s|$ smaller than ε within a short time and reduce chattering because \dot{K} exponentially decreases as $|s|$ goes to zero. \dot{K} intercepted at $|s| = 0$ can be adjusted by tuning β .

The proposed adaptive law is guaranteed to be UUB, which is proven in the Appendix.

B. SIMULATION SETUP

Several simulations were conducted to illustrate the performance of the proposed ASMC. The mathematical model of

a 2-DOF robot manipulator was provided by:

$$\begin{aligned} \mathbf{M}(\mathbf{q}) &= \begin{bmatrix} l_2^2 m_2 + 2l_1 l_2 m_2 c_2 + l_1^2 (m_1 + m_2) & l_2^2 m_2 + l_1 l_2 m_2 c_2 \\ l_2^2 m_2 + l_1 l_2 m_2 c_2 & l_2^2 m_2 \end{bmatrix} \end{aligned}$$

$$\begin{aligned} \mathbf{C}(\mathbf{q}, \dot{\mathbf{q}})\dot{\mathbf{q}} &= \begin{bmatrix} -m_2 l_1 l_2 s_2 \dot{q}_2^2 - 2m_2 l_1 l_2 s_2 \dot{q}_1 \dot{q}_2 \\ m_2 l_1 l_2 s_2 \dot{q}_2^2 \end{bmatrix} \end{aligned}$$

$$\begin{aligned} \mathbf{G}(\mathbf{q}) &= \begin{bmatrix} m_2 l_2 g c_{12} + (m_1 + m_2) l_1 g c_1 \\ m_2 l_2 g c_{12} \end{bmatrix}, \end{aligned}$$

$$\begin{aligned} \mathbf{F}(\dot{\mathbf{q}}) &= \begin{bmatrix} \alpha_1 \text{sgn}(\dot{q}_1) \\ \alpha_2 \text{sgn}(\dot{q}_2) \end{bmatrix} \end{aligned}$$

where q_i is the angle of joint i ; g denotes the gravitational acceleration; s_i , c_i , and c_{ij} are defined by $\sin(q_i)$, $\cos(q_i)$, and $\cos(q_i + q_j)$, respectively; and l_i , m_i , and α_i denote the i th link length, mass, and friction coefficient, respectively. The relevant parameters are set to be $m_1 = 9$ kg, $m_2 = 6$ kg, $l_1 = 0.4$ m, $l_2 = 0.2$ m, and $\alpha_1 = \alpha_2 = 40$. The control gain $\bar{M} = \text{diag}(0.08, 0.04)$ is chosen to satisfy $\|I - M^{-1}(q(t))\bar{M}\| < 1$ according to the inequality condition (8). Since the inertia matrix of a robot manipulator is a periodic function with a period of 2π , the inequality (8) can be guaranteed by ensuring it between 0 and 2π .

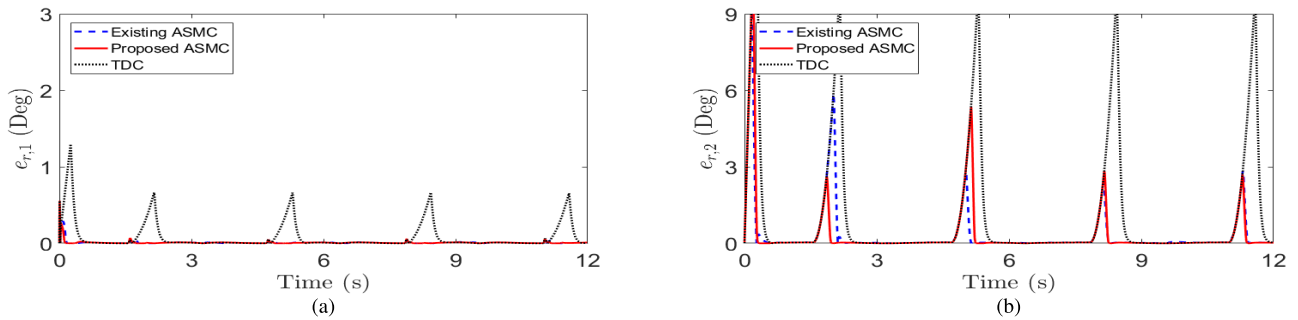


FIGURE 3. Nominal performance comparison in the joint space in terms of the tracking errors of the TDC without the ASMC (dotted line), the existing ASMC (dashed line), and the proposed ASMC (solid line) for joints (a) 1 and (b) 2.

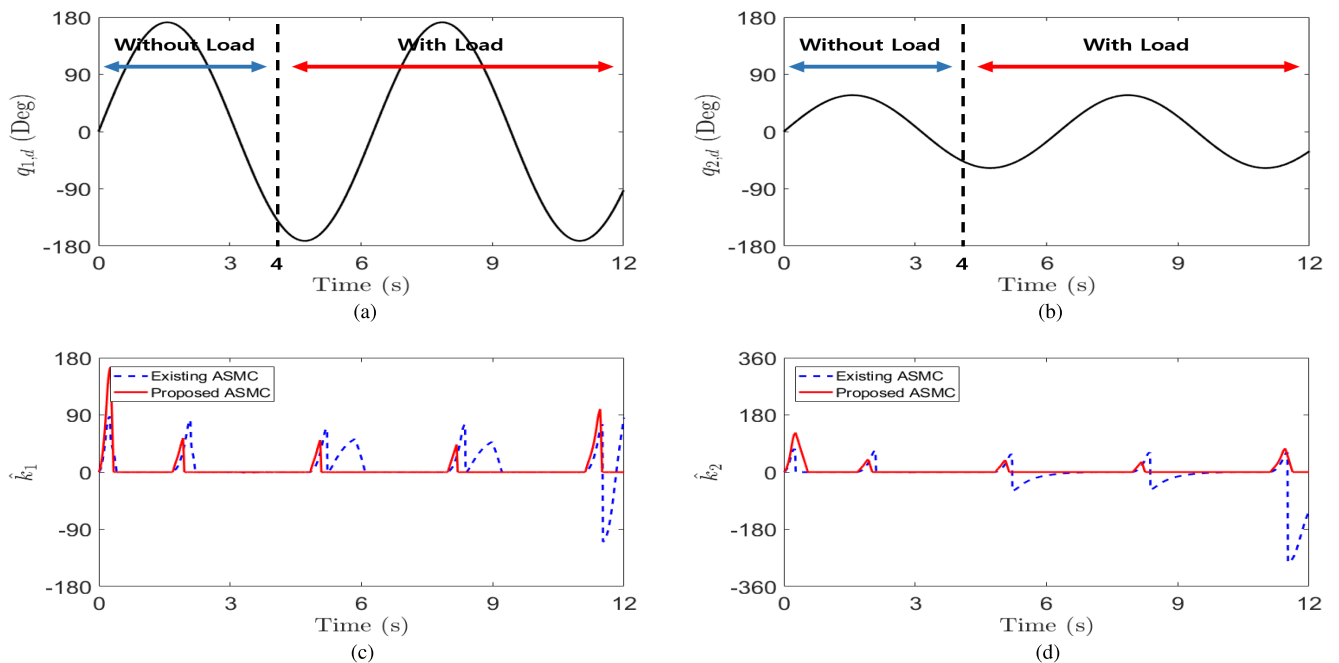


FIGURE 4. Comparison of the switching gains for the given reference angles in the joint space with payload carried after around 4 s: (a) reference angle of joint 1, (b) reference angle of joint 2, (c) switching gains of the proposed and existing ASMC for joint 1, and (d) switching gains of the proposed and existing ASMC for joint 2.

C. PERFORMANCE COMPARISON IN THE JOINT SPACE

The reference joint angle trajectories were given, and comparisons were made in terms of the tracking errors and the switching gains to illustrate the performance in the joint space. For comparison, the existing ASMC [16] was employed, and its parameters were best tuned for its maximum nominal performance. For the robust performance comparison, a payload of 3 kg was carried, and the control parameters tuned without payload were still adopted to evaluate the robust performance. The parameters in (9), (10), and (11) of the proposed ASMC were $K_s = \text{diag}(100, 100)$, $K_p = \text{diag}(15, 15)$, $\varphi_1 = 80$, $\gamma_1 = 2$, $\beta_1 = 10$, $\varphi_2 = 30$, $\gamma_2 = 1$, $\beta_2 = 10$, and $\varepsilon = 1$, and these parameters of the existing ASMC were $\varphi_1 = 80$, $\gamma_1 = 2$, $\varphi_2 = 100$, $\gamma_2 = 3$.

1) NOMINAL PERFORMANCE IN THE JOINT SPACE

For the given reference angles in the joint space in Figs. 2(a) and (b), the switching gains and the tracking errors of the proposed and existing ASMCs are compared in Figs. 2(c) and (d) and Figs. 3(a) and (b). When $|s|$ is smaller than ε (i.e., $|s| < \varepsilon$), the switching gains of the proposed and existing ASMCs are proportional to $1/|s|$ and $\beta_i e^{-|s_{i,t}|}$, respectively. This is why the proposed and existing ASMCs provide robustness to the TDE errors and have smaller tracking errors compared with the pure TDC (Fig. 3). Both of them show a fast adaptation speed and a similar nominal performance when no payload is present.

2) ROBUST PERFORMANCE IN THE JOINT SPACE

A payload of 3 kg was carried after approximately 4 s on the end-tip of a robot manipulator to demonstrate the robustness

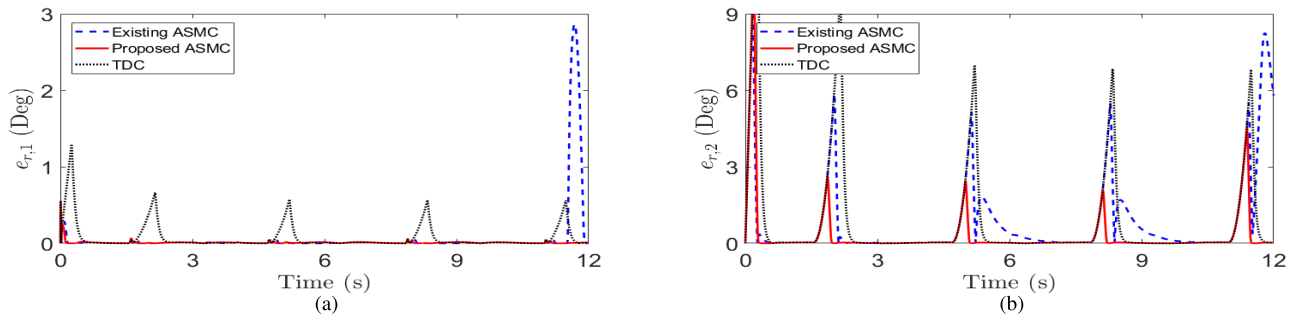


FIGURE 5. Robust performance comparison in the joint space in terms of the tracking errors of the TDC without ASMC (dotted line), the existing ASMC (dashed line), and the proposed ASMC (solid line) for joints (a) 1 and (b) 2.

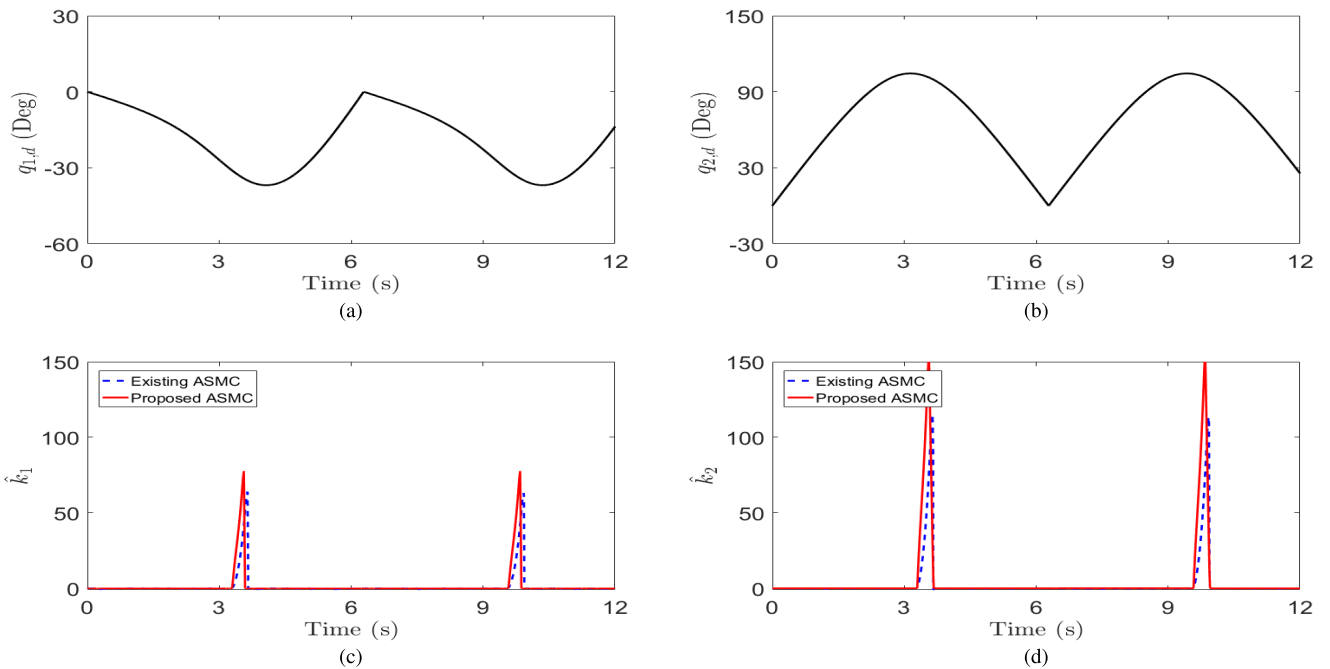


FIGURE 6. Comparison of the switching gains for the given reference angle in the joint space without payload: (a) reference angle of joint 1, (b) reference angle of joint 2, (c) switching gains of the proposed and existing ASMCs for joint 1, and (d) switching gains of the proposed and existing ASMCs for joint 2.

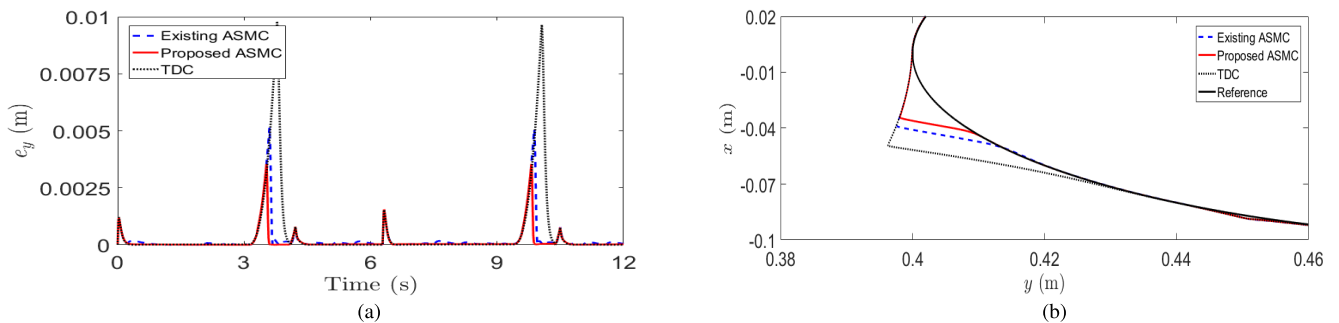


FIGURE 7. Nominal performance comparison in task space in terms of the tracking errors of the TDC without ASMC (dotted line), the existing ASMC (dashed line), and the proposed ASMC (solid line) for the (a) y-coordinate and (b) xy-coordinate.

of the proposed ASMC. The control parameters best-tuned without payload were still adopted to evaluate the robust performance. The moment that the payload was delivered,

the TDE errors immediately increased, and a larger switching gain was required to suppress them. It is highly probable that in the process of rapidly reducing the switching gains

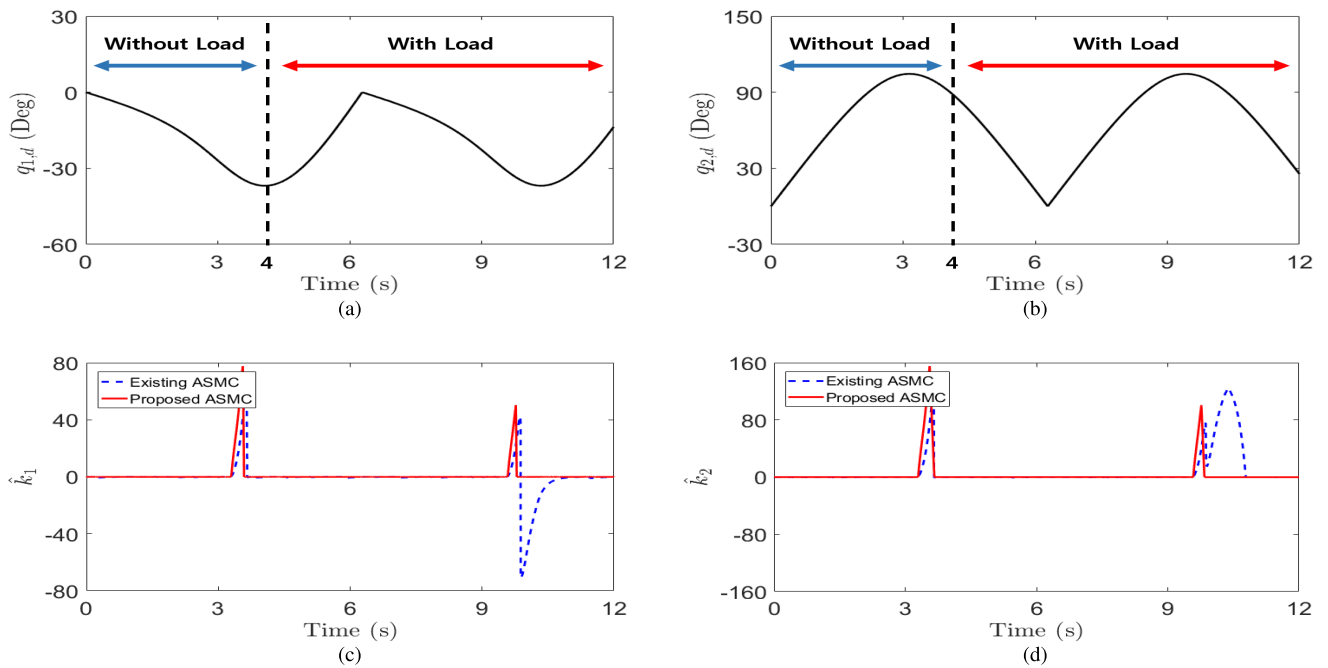


FIGURE 8. Comparison of the switching gains for the reference angles in the joint space with the payload carried for approximately 4 s: (a) reference angle of joint 1, (b) reference angle of joint 2, (c) switching gains of the proposed and existing ASMCs for joint 1, and (d) switching gains of the proposed and existing ASMCs for joint 2.

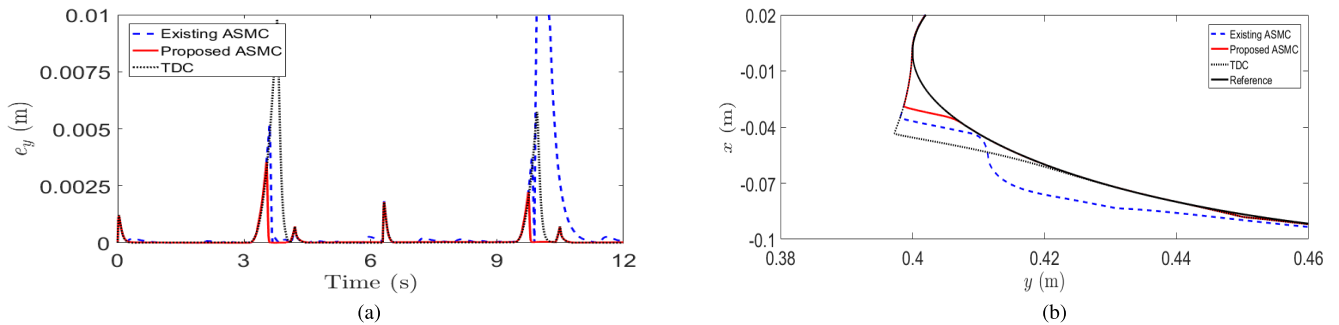


FIGURE 9. Robust performance comparison in task space in terms of the tracking errors of the TDC without ASMC (dotted line), the existing ASMC (dashed line), and the proposed ASMC (solid line) for the (a) y-coordinate and the (b) xy-coordinate.

near the sliding surface, excessive adaptation occurs in the existing ASMC; hence, its performance degrades. As seen in Figs. 4(c) and (d), the switching gains of the existing ASMC became temporarily negative because of their excessive adaptation caused by the payload carried after approximately 4 s, whereas those of the proposed ASMC were relatively insensitive to an external payload because of the adaptive law with a new term $\beta_i e^{-|s_{i,d}|}$. The proposed ASMC can be said to achieve the effective switching gain tuning. Fig. 5 shows that the proposed ASMC had a better robust performance. The large tracking error happened to the existing ASMC at 4 s, which was not the case with the proposed ASMC. We confirmed through simulation studies that the proposed ASMC can achieve a good tracking performance without excessive adaptation of the switching gains under uncertain systems.

D. PERFORMANCE COMPARISON IN TASK SPACE

The circular reference trajectory was given, and comparisons were made in terms of the tracking errors and the switching gains to illustrate the performance in task space. The corresponding reference angle trajectories were computed by inverse kinematics from the task space to the joint space. As in the comparison in the joint space, the existing ASMC [16] was employed for comparison, and its parameters were best tuned for its maximum nominal performance. In the same manner, a robust performance comparison was made by carrying a payload of 3 kg at 4s and adopting control parameters tuned without payload. The parameters in (9), (10), and (11) were chosen to be $K_s = \text{diag}(100, 100)$, $K_p = \text{diag}(15, 15)$, $\varphi_1 = 100$, $\gamma_1 = 2$, $\beta_1 = 10$, $\varphi_2 = 100$, $\gamma_2 = 1$, $\beta_2 = 10$, and $\varepsilon = 1$, and these parameters of the existing ASMC were $\varphi_1 = 100$, $\gamma_1 = 2$, $\varphi_2 = 90$, $\gamma_2 = 1$.

1) NOMINAL PERFORMANCE IN TASK SPACE

The circular reference trajectory in task space was transformed by inverse kinematics into angle trajectories of joints 1 and 2, as seen in Figs. 6(a) and (b). For the obtained reference angles in the joint space in Figs. 6(a) and (b), the switching gains and the tracking errors of the proposed and existing ASMCs were compared in Figs. 6(c) and (d) and Figs. 7(a) and (b). The tracking errors of the y and x-y coordinates in task space were represented in Figs. 7(a) and (b), respectively. A trajectory in Fig. 7(b) ranged from 10.3 to 11 s, which is a part of a full circular reference as seen inside a dotted box. As in comparison in the joint space, the proposed and existing ASMCs showed a similar nominal performance when no payload was present, and both of them were superior to the pure TDC because of their adaptive laws. Fig. 7(b) depicts that the pure TDC had steady-state tracking errors because of the TDE errors.

2) ROBUST PERFORMANCE IN TASK SPACE

A payload of 3 kg was carried at 4 s on the end-tip of a robot manipulator to demonstrate the robustness of the proposed ASMC in task space. As in comparison in the joint space, the control parameters best-tuned without payload were still adopted to evaluate the robust performance. Overall, the results in task space had a similar tendency with those in the joint space. Fig. 8 shows that the switching gain of joint 1 became negative because of the excessive adaptation near the sliding surface and also caused large switching gains of joint 2. In contrast, the proposed ASMC was relatively insensitive to an external payload because of the adaptive law with a new term $\beta_i e^{-|s_{i,t}|}$. Therefore, the proposed ASMC can be said to achieve the effective switching gain tuning. Fig. 9 shows the tracking errors of the proposed ASMC, the existing ASMC, and the pure TDC with a payload carried at 4 s. The proposed ASMCs are designed to preserve good tracking performance even for uncertain systems by suppressing TDE errors effectively. Robust tracking performance of the proposed ASMCs are illustrated in Fig. 9 which shows the tracking errors with a payload carried from 10 s to 11 s. It can be seen that the proposed ASMC still keeps the good tracking performance even though payload is applied. This is why the proposed ASMCs are said to be robust to uncertainties.

IV. CONCLUSION

This study proposed a new practical adaptive law applied to ASMC for nonlinear dynamic systems to achieve effective switching gain tuning near the sliding surface and offer chattering reduction as well as fast adaptation speed. By employing the negative exponential of the magnitude of the sliding variable near the sliding surface instead of its inverse, the proposed ASMC alleviated the inherent trade-off between chattering and tracking performance without undesirable side effects. Simulation studies have shown that the proposed ASMC has a better robust performance in joint and task spaces than existing control schemes without suffering from

chattering. The proposed ASMC was motivated by practical implementation when applying to relatively poor hardware systems. Many other industrial applications with low-cost hardware will be waiting to be developed with the proposed ASMC.

APPENDIX

A. STABILITY ANALYSIS

Consider a Lyapunov function as:

$$V_t = \frac{1}{2} s_t^T s_t + \frac{1}{2} \sum_{i=1}^n \frac{\gamma_i}{\varphi_i} \tilde{k}_{i,t}^2 \tag{12}$$

where $\tilde{k}_{i,t} = \bar{h}_i^* - \hat{k}_{i,t}$, and \bar{h}_i^* is the upper bound of TDE errors Differentiating the Lyapunov function (12) with respect to time t and substituting (9) into (12) yield:

$$\begin{aligned} \dot{V}_t &= s_t^T \dot{s}_t - \sum_{i=1}^n \frac{\gamma_i}{\varphi_i} \tilde{k}_{i,t} \dot{\tilde{k}}_{i,t} \\ &= s_t^T (\ddot{e}_t + K_s \dot{e}_t) - \sum_{i=1}^n \frac{\gamma_i}{\varphi_i} \tilde{k}_{i,t} \dot{\tilde{k}}_{i,t} \end{aligned} \tag{13}$$

Substituting (2), (5), and (10) into (13), we obtain:

$$\begin{aligned} \dot{V}_t &= s_t^T (\ddot{x}_{d,t} - \ddot{x}_t + K_s \dot{e}_t) - \sum_{i=1}^n \frac{\gamma_i}{\varphi_i} \tilde{k}_{i,t} \dot{\tilde{k}}_{i,t} \\ &= s_t^T (\ddot{x}_{d,t} - \ddot{h}_t - \bar{b}^{-1} \ddot{u}_t + K_s \dot{e}_t) - \sum_{i=1}^n \frac{\gamma_i}{\varphi_i} \tilde{k}_{i,t} \dot{\tilde{k}}_{i,t} \\ &= s_t^T (-(h_t - h_{t-L}) - K_p s_t - \hat{K}_t \text{sgn}(s_t)) - \sum_{i=1}^n \frac{\gamma_i}{\varphi_i} \tilde{k}_{i,t} \dot{\tilde{k}}_{i,t} \\ &\leq \sum_{i=1}^n |s_{i,t}| \bar{h}_i^* - \sum_{i=1}^n k_{p,i} s_{i,t}^2 - \sum_{i=1}^n \hat{k}_{i,t} |s_{i,t}| - \sum_{i=1}^n \frac{\gamma_i}{\varphi_i} \tilde{k}_{i,t} \dot{\tilde{k}}_{i,t} \\ &\leq \sum_{i=1}^n |s_{i,t}| \tilde{k}_{i,t} - \sum_{i=1}^n k_{p,i} s_{i,t}^2 - \sum_{i=1}^n \frac{\gamma_i}{\varphi_i} \tilde{k}_{i,t} \dot{\tilde{k}}_{i,t} \end{aligned} \tag{14}$$

Consider two cases: $|s_t|_\infty > \varepsilon$ and $|s_t|_\infty < \varepsilon$. In the case of $|s_t|_\infty > \varepsilon$, by substituting (11) into (14), we obtain:

$$\begin{aligned} \dot{V}_t &\leq \sum_{i=1}^n |s_{i,t}| \tilde{k}_{i,t} - \sum_{i=1}^n k_{p,i} s_{i,t}^2 - \sum_{i=1}^n \tilde{k}_{i,t} (|s_{i,t}| + \beta_i e^{-|s_{i,t}|}) \\ &\leq \sum_{i=1}^n |s_{i,t}| \tilde{k}_{i,t} - \sum_{i=1}^n k_{p,i} s_{i,t}^2 \end{aligned} \tag{15}$$

According to the Lemma in [16], the switching gain $\hat{k}_{i,t}$ can be chosen to be

$$\hat{k}_{i,t} \leq \bar{h}_i^* \tag{16}$$

then we obtain:

$$\dot{V}_t \leq - \sum_{i=1}^n k_{p,i} s_{i,t}^2 \tag{17}$$

which means that V_t is decreasing and bounded because $0 \leq V_t \leq V_0 < \infty$, and $|s_t|_\infty$ arrives at the region $|s_t|_\infty < \varepsilon$ within a finite time $t_\varepsilon > 0$.

Although s_t enters into the region $|s_t|_\infty < \varepsilon$ within a finite time, it may go inside and outside its boundary because \dot{V}_t is not guaranteed to be non-positive inside. If s_t leaves the region $|s_t|_\infty < \varepsilon$, the sign of \dot{V}_t becomes negative again according to (17), which makes it enter the sliding surface.

The Lyapunov function V_t in (12) is bounded as follows if s_t enters into the region $|s_t|_\infty < \varepsilon$:

$$\frac{1}{2}|s_t|_2^2 \leq V_t \leq \frac{1}{2}|s_t|_2^2 + \frac{1}{2} \sum_{i=1}^n \frac{\gamma_i}{\varphi_i} \tilde{k}_{i,t}^2 \quad (18)$$

where $\frac{1}{2} \sum_{i=1}^n \frac{\gamma_i}{\varphi_i} \tilde{k}_{i,t}^2$ is bounded because \bar{h}_i^* is constant, and $\hat{k}_{i,t}$ is bounded according to Lemma in [16]. It follows then that we have:

$$V_t < \frac{1}{2} \sum_{i=1}^n \varepsilon^2 + \frac{1}{2} \sum_{i=1}^n \tilde{k}_M \quad (19)$$

where \tilde{k}_M is the maximum value of $\sum_{i=1}^n \frac{\gamma_i}{\varphi_i} (\bar{h}_i^* - \hat{k}_{i,t})^2$

Putting (18) and (19) together yields:

$$|s_t|_2 < \sqrt{\sum_{i=1}^n \varepsilon^2 + \sum_{i=1}^n \tilde{k}_M} \quad (20)$$

which means that s_t is UUB for $t \leq t_\varepsilon$. The fluctuation of the sliding variable s_t near the small vicinity of the sliding surface is guaranteed to be upper-bounded by (20).

In summary, s_t was bounded, and the error dynamics $\dot{e}_t = -K_s e_t$ was asymptotically stable. The system was guaranteed to be bounded input and bounded output (BIBO) stable [25].

REFERENCES

- [1] V. Utkin, J. Guldner, and J. Shi, *Sliding Mode Control in Electro-Mechanical Systems*. Boca Raton, FL, USA: CRC Press, 2009.
- [2] M. S. Park and D. Chwa, "Swing-up and stabilization control of inverted-pendulum systems via coupled sliding-mode control method," *IEEE Trans. Ind. Electron.*, vol. 56, no. 9, pp. 3541–3555, Sep. 2009.
- [3] S. Islam and X. P. Liu, "Robust sliding mode control for robot manipulators," *IEEE Trans. Ind. Electron.*, vol. 58, no. 6, pp. 2444–2453, Jun. 2011.
- [4] S. Di Gennaro, J. R. Domínguez, and M. A. Meza, "Sensorless high order sliding mode control of induction motors with core loss," *IEEE Trans. Ind. Electron.*, vol. 61, no. 6, pp. 2678–2689, Jun. 2014.
- [5] A. Levant, "Principles of 2-sliding mode design," *Automatica*, vol. 43, no. 4, pp. 576–586, Apr. 2007.
- [6] C. J. Fallaha, M. Saad, H. Y. Kanaan, and K. Al-Haddad, "Sliding-mode robot control with exponential reaching law," *IEEE Trans. Ind. Electron.*, vol. 58, no. 2, pp. 600–610, May 2011.
- [7] O. Barambones and P. Alkorta, "Position control of the induction motor using an adaptive sliding-mode controller and observers," *IEEE Trans. Ind. Electron.*, vol. 61, no. 12, pp. 6556–6565, Dec. 2014.
- [8] H. Lee and V. I. Utkin, "Chattering suppression methods in sliding mode control systems," *Annu. Rev. Control*, vol. 31, no. 2, pp. 179–188, 2007.
- [9] M.-L. Tseng and M.-S. Chen, "Chattering reduction of sliding mode control by low-pass filtering the control signal," *Asian J. Control*, vol. 12, no. 3, pp. 392–398, May 2010.
- [10] Y.-J. Huang, T.-C. Kuo, and S.-H. Chang, "Adaptive sliding-mode control for nonlinear systems with uncertain parameters," *IEEE Trans. Syst., Man, Cybern. B, Cybern.*, vol. 38, no. 2, pp. 534–539, Apr. 2008.
- [11] V. Bregeault, V. Brégeault, F. Plestan, Y. Shtessel, and A. Poznyak, "Adaptive sliding mode control for an electropneumatic actuator," in *Proc. 11th Int. Workshop Variable Struct. Syst. (VSS)*, Jun. 2010, pp. 260–265.
- [12] F. Plestan, Y. Shtessel, V. Brégeault, and A. Poznyak, "Sliding mode control with gain adaptation—Application to an electropneumatic actuator," *Control Eng. Pract.*, vol. 21, no. 5, pp. 679–688, May 2013.
- [13] Z. Man, M. O'Day, and X. Yu, "A robust adaptive terminal sliding mode control for rigid robotic manipulators," *J. Intell. Robot. Syst.*, vol. 24, no. 1, pp. 23–41, Jan. 1999.
- [14] S.-Y. Chen and F.-J. Lin, "Robust nonsingular terminal sliding-mode control for nonlinear magnetic bearing system," *IEEE Trans. Control Syst. Technol.*, vol. 19, no. 3, pp. 636–643, May 2011.
- [15] M. B. R. Neila and D. Tarak, "Adaptive terminal sliding mode control for rigid robotic manipulators," *Int. J. Automat. Comput.*, vol. 8, no. 2, pp. 215–220, May 2011.
- [16] J. Baek, M. Jin, and S. Han, "A new adaptive sliding-mode control scheme for application to robot manipulators," *IEEE Trans. Ind. Electron.*, vol. 63, no. 6, pp. 3628–3637, Jun. 2016.
- [17] S. Roy, I. N. Kar, J. Lee, and M. Jin, "Adaptive-robust time-delay control for a class of uncertain Euler–Lagrange systems," *IEEE Trans. Ind. Electron.*, vol. 64, no. 9, pp. 7109–7119, Sep. 2017.
- [18] S.-J. Cho, M. Jin, T.-Y. Kuc, and J. S. Lee, "Stability guaranteed auto-tuning algorithm of a time-delay controller using a modified Nussbaum function," *Int. J. Control*, vol. 87, no. 9, pp. 1926–1935, Feb. 2014.
- [19] M. Jin, S. H. Kang, and P. H. Chang, "Robust compliant motion control of robot with nonlinear friction using time-delay estimation," *IEEE Trans. Ind. Electron.*, vol. 55, no. 1, pp. 258–269, Jan. 2008.
- [20] K. Youcef-Toumi and O. Ito, "A time delay controller for systems with unknown dynamics," *J. Dyn. Syst., Meas., Control*, vol. 112, no. 1, pp. 133–142, Mar. 1990.
- [21] T. C. S. Hsia, T. A. Lasky, and Z. Guo, "Robust independent joint controller design for industrial robot manipulators," *IEEE Trans. Ind. Electron.*, vol. 38, no. 1, pp. 21–25, Feb. 1991.
- [22] Y.-X. Wang, D.-H. Yu, and Y.-B. Kim, "Robust time-delay control for the DC–DC boost converter," *IEEE Trans. Ind. Electron.*, vol. 61, no. 9, pp. 4829–4837, Sep. 2014.
- [23] M. Jin, J. Lee, and K. K. Ahn, "Continuous nonsingular terminal sliding-mode control of shape memory alloy actuators using time delay estimation," *IEEE/ASME Trans. Mechatronics*, vol. 20, no. 2, pp. 899–909, Apr. 2015.
- [24] M. Spong and M. Vidyasagar, "Robust linear compensator design for nonlinear robotic control," *IEEE J. Robot. Autom.*, vol. RA-3, no. 4, pp. 345–351, Aug. 1987.
- [25] K. M. Hangos, J. Bokor, and G. Szederkényi, *Analysis and Control of Nonlinear Process Systems*. New York, NY, USA: Springer, 2006.



SEUNGMIN BAEK received the B.S. degree in electrical engineering from the Pohang University of Science and Technology, Pohang, South Korea, in 2018, where he is currently pursuing the Ph.D. degree (M.S.–Ph.D. Joint Program) in creative IT engineering.

His main research interests include controller design for industrial systems, robot manipulator, and robust control of nonlinear systems.



JAEMIN BAEK (S'16–M'18) received the B.S. degree in mechanical engineering from Korea University, Seoul, South Korea, in 2011, and the Ph.D. degree (M.S.–Ph.D. Joint Program) in creative IT engineering from the Pohang University of Science and Technology, in 2018. Since 2018, he has been with the Defense Satellite Systems PMO, Agency for Defense Development, Daejeon, South Korea.

His main research interests include controller design for industrial systems, control system designs, and robust controls.



SOOHEE HAN (M'12–SM'13) received the B.S. degree in electrical engineering from Seoul National University (SNU), Seoul, South Korea, in 1998, and the M.S. and Ph.D. degrees from the School of Electrical Engineering and Computer Science, SNU, in 2000 and 2003, respectively. From 2003 to 2007, he was a Researcher with the Engineering Research Center for Advanced Control and Instrumentation, SNU. In 2008, he was a Senior Researcher with the Robot S/W Research

Center. From 2009 to 2014, he was with the Department of Electrical Engineering, Konkuk University, Seoul. Since 2014, he has been with the Department of Creative IT Engineering, POSTECH, Pohang, South Korea.

His main research interests include the areas of computer-aided control system designs, distributed control systems, time-delay systems, and stochastic signal processing.

• • •